

Non-annular, hemispheric signature of the winter North Atlantic Oscillation

J. García-Serrano¹ · R. J. Haarsma²

Received: 24 November 2015 / Accepted: 19 July 2016 / Published online: 26 July 2016
© Springer-Verlag Berlin Heidelberg 2016

Abstract Sensitivity experiments with an atmospheric general circulation model (AGCM) without a proper stratosphere are performed to locally force a North Atlantic oscillation (NAO)-like response in order to analyse the tropospheric dynamics involved in its hemispheric extent. Results show that the circulation anomalies are not confined to the North Atlantic basin not even within the first 10 days of integration, where the atmospheric response propagates downstream into the westerly jets. At this linear stage, transient-eddy activity dominates the emerging, regional NAO-like pattern while zonal-eddy coupling may add on top of the wave energy propagation. Later at the quasi-equilibrium nonlinear stage, the atmospheric response emphasizes a wavenumber-5 structure embedded in the westerly jets, associated with transient-eddy feedback upon the Atlantic and Pacific storm-tracks. This AGCM waveguided structure rightly projects on the observational NAO-related circumglobal pattern, providing evidence of its non-annular character in the troposphere. These findings support the view on the importance of the circumglobal waveguide pattern on the development of NAO-related anomalies at hemispheric level. It could help to settle a consensus view of the Arctic Oscillation, which has been elusive so far.

Keywords Winter NAO · Circumglobal waveguide pattern · Non-annular teleconnection

1 Introduction

The North Atlantic Oscillation (NAO) largely dominates atmospheric variability during Euro-Atlantic winter and its associated impacts govern, likewise, climate variability in the North Atlantic surrounding areas (e.g. Hurrell et al. 2003; Hurrell and Deser 2009). In recent years, there has been a relevant increase in understanding the dynamics involved in the NAO. It is well established that the NAO can be regarded as the main integrator of fluctuations in the Atlantic storm-track and the associated eddy-driven jet (e.g. Thompson et al. 2003; Vallis and Gerber 2008; Gerber and Vallis 2009; Wettstein and Wallace 2010), being tied to breaking of synoptic-scale Rossby waves (e.g. Rivière and Orlanski 2007; Strong and Magnusdottir 2008; Woollings et al. 2008) that links blocking occurrence with weather regimes (e.g. Woollings et al. 2010; Davini et al. 2012).

The internal, regional dynamics of the NAO variability is supported by the confinement of the pattern to the North Atlantic basin at lower-tropospheric levels (e.g. García-Serrano et al. 2011); although, it is recognized that weaker anomalies in phase with North Atlantic mid-latitudes are systematically present in the North Pacific basin (e.g. Hurrell et al. 2003). This latter quasi-zonally symmetric appearance led to the paradigm of the Arctic Oscillation or Northern Annual Mode (AO/NAM) (Thompson and Wallace 1998, 2000, 2001). The AO/NAM variability relies on a large-scale seesaw in atmospheric mass between middle and high latitudes, which is thought to have a deep barotropic, annular signature throughout the atmosphere (Thompson et al. 2003). In contrast, the variability

Electronic supplementary material The online version of this article (doi:10.1007/s00382-016-3292-3) contains supplementary material, which is available to authorized users.

✉ J. García-Serrano
javier.garcia@bsc.es

¹ Earth Sciences Department, Barcelona Supercomputing Center (BSC-CNS), Barcelona, Spain

² Koninklijk Nederlands Meteorologisch Instituut (KNMI), De Bilt, The Netherlands

associated with the NAO-AO has a distinct hemispheric pattern at upper-tropospheric levels, which is wave-like (Nigam 2003; Thompson et al. 2003). This hemispheric signature was identified by Branstator (2002) as embedded in the circumglobal waveguide pattern (CWP), which has non-annular, zonally-propagating Rossby wave dynamics (Hoskins and Ambrizzi 1993). The NAO/CWP paradigm provides a quasi-zonally symmetric structure at surface (García-Serrano et al. 2011), since the waveguide pattern tends to vanish at low levels over continents (Branstator 2002), thereby may reconcile the debate about the Pacific centre of action in the NAO-related variability (e.g. Deser 2000; Wallace 2000; Ambaum et al. 2001; Dommenget and Latif 2002; Wallace and Thompson 2002; Huth 2006) but maintaining a non-annular behaviour (c.f. Cohen and Saito 2002; Feldstein and Franzke 2006).

In the middle troposphere (500 hPa), the NAO-related atmospheric variability shows two centres of action in the North Pacific and the one at North Atlantic mid-latitudes, still more pronounced, elongates resembling another two centres of action (e.g. Baldwin et al. 1994; Christiansen 2002; Woollings et al. 2010). The same hemispheric anomalies can be found in the upper troposphere (e.g. DeWeaver and Nigam 2000a, b), in the tropopause height (Ambaum and Hoskins 2002) or just above the tropopause level (Baldwin et al. 2003). The fifth centre of action of the NAO/CWP pattern is located around the Arabian Peninsula (Branstator 2002). The NAO-related wavenumber-5 structure at upper-tropospheric levels is better displayed in the streamfunction field or the rotational (non-divergent) component of the meridional wind (e.g. Branstator 2002; García-Serrano et al. 2011), presumably because its dynamics invokes Rossby wave propagation into the westerly jets.

Further upward into the stratosphere, the atmospheric variability becomes more zonal (e.g. Thompson and Wallace 2000) and the NAM-like variability gains more dynamical significance (e.g. Vallis and Gerber 2008). Interestingly, observational and modelling studies show that changes in the stratospheric polar vortex strength lead to a regional NAO-like pattern at surface rather than to an AO/NAM-like signature (e.g. Baldwin and Dunkerton 2001; Ambaum and Hoskins 2002; Norton 2003; Shaw et al. 2014), with mid-tropospheric anomalies projecting on the CWP structure (e.g. Kindem and Christiansen 2001; Christiansen 2002). The troposphere-stratosphere covariability is, likewise, associated with a near-surface circulation anomaly that is most pronounced in the North Atlantic basin (e.g. Perlwitz and Graf 1995; Baldwin et al. 2003), but involving a non-annular, hemispheric NAO/CWP-like pattern aloft (e.g. Baldwin et al. 1994, 2003; Ambaum and Hoskins 2002). Hence, even considering the NAO-related troposphere-stratosphere coupling as a regional

phenomenon (e.g. Ambaum and Hoskins 2002; Davini et al. 2014), it yields circumglobal circulation anomalies apparently trapped into the westerly jets.

The physical relationship between the regional NAO and the hemispheric AO, defined at surface, is not well established. The starting point of this study is the NAO/CWP paradigm in the troposphere. The purpose is to explore whether tropospheric dynamics can explain the establishment of NAO-related anomalies at hemispheric level, particularly the Pacific centre of action in the NAO-AO-related variability. To this aim, an AGCM without a proper stratosphere is used to force, regionally, a NAO-like response and to analyse the development of the associated CWP-like pattern.

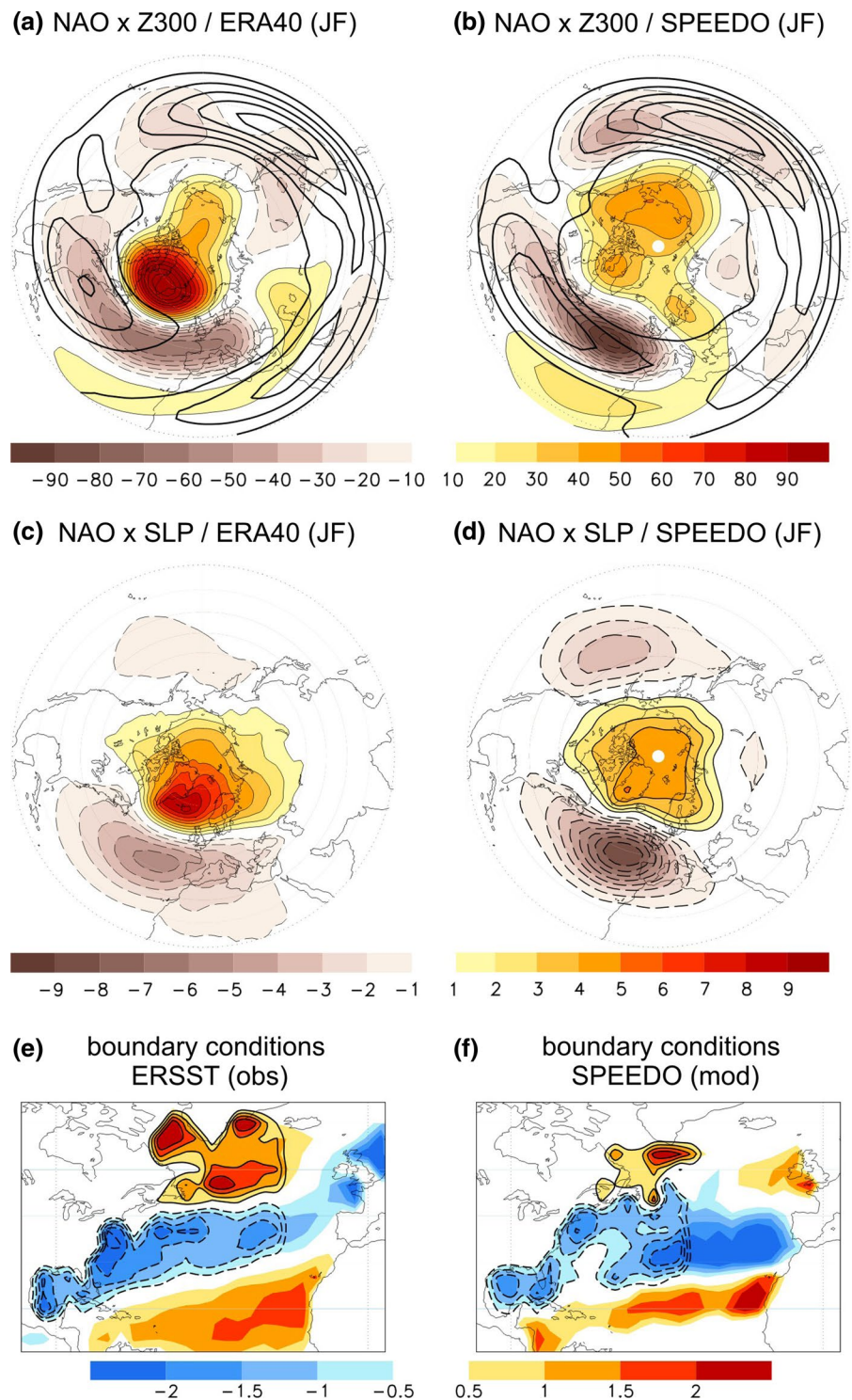
2 Model and experimental setup

The atmosphere model used in this study is the Simplified Parameterizations primitive-Equation DYNAMICS (SPEEDY) model (Molteni 2003). It is an intermediate complexity AGCM based on a spectral primitive equation core and a set of simplified parameterization schemes, which were especially designed to work in models with just a few vertical levels but are similar to those adopted in state-of-the-art AGCMs. SPEEDY has a vertical resolution of seven layers and a triangular spectral truncation at total wavenumber 30 (i.e. T30L7). The levels correspond to 925, 850, 700, 500, 300, 200, and 100 hPa. SPEEDY has a good damping parameterization in the upper-most level that allows absorption of waves and prevents spurious reflection (Fred Kucharski, personal communication; see also King et al. 2010). A five-layer version of the model is described in detail by Molteni (2003). The seven-layer version improved climate and is described and validated in Hazeleger et al. (2003) and Bracco et al. (2004); see Kucharski et al. (2013) for updates.

In order to obtain sea surface temperature (SST) forcing fields for the AGCM sensitivity experiments, a coupled run is firstly analysed. The coupled model SPEEDO (SPEEDY-Ocean) was configured for the Atlantic basin from 45°S to 60°N, with restoring conditions of the thermodynamic properties applied at the northern and southern boundaries; outside the Atlantic and over land climatological surface temperature was prescribed (e.g. Hazeleger and Haarsma 2005; Haarsma et al. 2005, 2008). The ocean component consisted of the Miami Isopycnic Coordinate Ocean Model (MICOM) version 2.7 (Bleck et al. 1992). SPEEDO was integrated for 60 years from which the last 50 years are used for analysis (Haarsma et al. 2005).

A set of sensitivity experiments with SPEEDY have been performed in this study, namely control (CTL) and perturbed runs, both consisting of 200-member ensembles

Fig. 1 Regression map of ERA40 (a, c) and SPEEDY-MICOM (SPEEDO; b, d) Z300 (m; *top*) and SLP (hPa; *middle*) anomalies in January–February onto the corresponding NAO index. Overplotted in *top panels* is the corresponding climatological zonal wind at 300 hPa ($c_i = 10 \text{ ms}^{-1}$ starting in 20 ms^{-1}). Contours in *bottom panels* delimit the forcing fields (SST anomalies; $^{\circ}\text{C}$) of the AGCM runs



of 30-day integrations for the month of January. The initial conditions for the first of January were obtained from a 200-year integration with climatological SSTs. The CTL transient simulations use SST climatology as boundary condition. In the perturbed transient simulations, a SST anomaly pattern is prescribed in the North Atlantic with climatology elsewhere. To partially separate results

from the model framework, and for ease of comparison, observational SSTs (ERSST; Smith et al. 2008) are also used in addition to SPEEDO SSTs. The anomalous forcing fields are shown in Fig. 1 (bottom), and correspond to the regression of ERSST anomalies onto the observational NAO index (Fig. 1e), as given by the ERA-40 re-analysis (Uppala et al. 2005), and SPEEDO SST anomalies onto the

model NAO index (Fig. 1f). Principal component analysis (PCA/EOF; von Storch and Zwiers 2001) has been applied upon monthly sea level pressure (SLP) anomalies over 90°W – 40°W / 20°N – 90°N to obtain the corresponding NAO index; the target season is January–February (García-Serrano et al. 2011). The amplitude of the SST regression maps have been amplified to reach a maximum of 2.5°C (Fig. 1-bottom), similar to previous studies (e.g. Kucharski and Molteni 2003), in order to compensate the damping in surface heat flux as consequence of considering the sea as an infinite reservoir of heat capacity (AGCM simulations). Note that the forcing fields are restricted to a SST dipole in the western North Atlantic (Fig. 1-bottom, black contours), with the aim of inducing changes primarily in the eddy-driven jet and avoiding continuous baroclinic effects from the subtropical part (Li and Conil 2003); previous works have shown efficiency of the SST dipole in triggering a NAO-like response (Ferreira and Frankignoul 2005; Deser et al. 2007).

Analysis reveals that SPEEDO SST forcing yields identical atmospheric response as to ERSST anomalies (not shown), indicating that small-scale details in the boundary conditions are not determinant for SPEEDY; the results shown below are those from the observational SST anomaly (Fig. 1e). The focus here is not on the NAO-related SST feedback onto the North Atlantic atmosphere, which is well documented, but on the establishment of the circumglobal pattern associated with a SST-forced NAO-like response. The length of the transient simulations (30 days) is not enough to reach the equilibrium stage, with a strong barotropic structure, which takes about 2–3 months (e.g. Ferreira and Frankignoul 2005; Deser et al. 2007; see Fig. S5). Results additionally reveal that the atmospheric response is quite linear and does not substantially differ in NAO^- (to Fig. 1e), shown and discussed throughout the manuscript, from NAO^+ (to a SST anomaly opposite in sign to Fig. 1e); the transient response (until day 10 of integration) towards NAO^+ can be found in the supplementary material (Fig. S6). The size of the ensembles is 200, which ensures reducing internal (chaotic) variability and obtaining robust results. The forced atmospheric anomalies, hereafter referred to as *ensemble-mean response*, are estimated as the difference between the ensemble-mean of the perturbed and CTL runs. All anomalies discussed below are statistically significant at 95 % confidence level according to both, a *t* test of equal mean (von Storch and Zwiers 2001) and a *F*-test for the signal-to-noise ratio (Annamalai et al. 2007).

3 The NAO/CWP

The structure of the observed NAO is well known (e.g. Hurrell et al. 2003; Hurrell and Deser 2009). Figure 1c

shows the global SLP regression map of the ERA-40 NAO index in mid-winter (January–February; see also García-Serrano et al. 2011); note that its negative phase is displayed (NAO^-). The canonical pattern is dominated by a strong meridional dipole between middle and high latitudes of the North Atlantic (i.e. the NAO), but usually includes weaker anomalies in the North Pacific (see Sect. 1); this signature is evident across different re-analyses and/or seasons considered (e.g. Deser 2000; Ambaum et al. 2001).

At mid/upper-tropospheric levels, the hemispheric anomalies associated with the observational NAO depicts a characteristic pattern as well; generally, with two weak centres of action in the North Pacific basin and an elongated one at North Atlantic mid-latitudes, projecting on two, embedded in the NAO-related dipole with high latitudes (e.g. Thompson et al. 2003; Woollings et al. 2010). Figure 1a points out this signature, showing the regression map of geopotential height at 300 hPa (Z300) onto the ERA-40 NAO^- index. These four apparent centres of action are distributed along the CWP pattern (Branstator 2002) and may, particularly the two over the North Pacific, reflect a stationary, zonally-propagating Rossby wavetrain (Hsu and Lin 1992; Hoskins and Ambrizzi 1993) triggered from the North Atlantic basin (Watanabe 2004; Watanabe and Jin 2004). The waveguide effect of the westerly jets is illustrated here by the collocation of the anomalies within the climatological zonal wind (Fig. 1a, thick contours). The fifth centre of action in the wavenumber-5 structure of the NAO/CWP pattern is located around the Arabian Peninsula, which becomes more noticeable in the streamfunction field (Fig. S1; Branstator 2002; García-Serrano et al. 2011).

The global SLP regression map of the model NAO^- index is displayed in Fig. 1d. As also shown in other AGCMs, SPEEDY overestimates the amplitude of the North Pacific centre of action related to the NAO at surface. At the upper troposphere, the regression map of Z300 (Fig. 1b) remains showing an overestimation of the NAO-related anomalies in the central-eastern North Pacific (see also the streamfunction anomalies in Fig. S1). This feature might be associated with the overestimated local wind maxima (Fig. 1a, b, thick contours) and more vigorous transient-eddy activity (Figs. 5b, c, 6d, thick contours) there as compared to the North Atlantic (cf. Vallis and Gerber 2008; Gerber and Vallis 2009). On the contrary, SPEEDY underestimates the amplitude of the centre of action at high latitudes (Fig. 1b, d). This latter could be linked to the fact that SPEEDY does not have a proper, active stratosphere (see Sect. 2), in that coupling processes and feedbacks (e.g. Ambaum and Hoskins 2002) are underrepresented.

Beyond biases, SPEEDY rightly captures both the NAO-related quasi-zonally symmetric signature at surface (Fig. 1d) and the wavenumber-5 structure at the upper troposphere (Fig. 1b), which projects on the observational one

(Fig. 1a; spatial correlation of 0.73). The hypothesis here is that the hemispheric scale of the NAO is non-annular in origin, namely the NAO/CWP could be at the basis of the AO development, implying that tropospheric dynamics is key for its circumglobal extent. This is assessed in Sect. 4.

The two lobes per basin of the NAO/CWP pattern collocate with the entrance- and exit-region of the corresponding jetstream. The basis of this configuration is beyond the scope of this study, and a more theoretical framework to address the question is required. It is noted, however, that the centres of action at the exit-regions, where the barotropic processes are more intense (e.g. Vallis and Gerber 2008; Gerber and Vallis 2009), are those penetrating to the surface (Fig. 1a–d); whereas the centres of action at the entrance-regions, where the baroclinic processes are dominant, are closer to continents (Branstator 2002). The fifth centre of action is at the interplay between the North African and Asian jets (Fig. 1a, b), where there is a relative maximum in the Eady growth rate (e.g. Vallis and Gerber 2008; Gerber and Vallis 2009).

4 Model circumglobal response

The transient and quasi-equilibrium ensemble-mean circulation anomalies towards NAO⁻ in response to SST anomalies in Fig. 1e are shown and discussed in the following (see Sect. 2).

At day 1 of integration (Fig. S2a, b), there is already a baroclinic response, albeit weak, at the core-region of the North Atlantic jet. This baroclinic structure, with positive geopotential height anomalies at lower levels (Z925) and negative ones at upper levels (Z300), remains until day 10 of integration but increasing in amplitude and extent (Fig. 2). The available energy into the system is indeed provided by the baroclinic processes associated with changes in the meridional temperature gradient induced by the anomalous SST forcing (Fig. 1e); here illustrated with the Eady growth rate at 850 hPa (Fig. 3-right), which measures baroclinic instability and governs the amplitude of the atmospheric perturbations (e.g. Hoskins and Valdes 1990). The ensemble-mean response at day 2 of integration covers the whole Atlantic basin, from the Gulf of Mexico to offshore Iberian Peninsula (Fig. 2a, b). At day 4, the circulation anomalies penetrate into Europe, with the upper-tropospheric anomalies (Fig. 2c) going slightly ahead than the lower-tropospheric anomalies (Fig. 2d). When the atmospheric anomalies are well developed over Europe at day 6 of integration, particularly for Z300 (Fig. 2e), the ensemble-mean response shows a barotropic anomaly at the exit-region of the North Pacific jet (Fig. 2e, f). This is striking, as no clear geopotential height anomalies propagating downstream, thus connecting the two regions, have

been shown. It is to note, however, that 1 day before (day 5) the atmospheric response displays a cyclonic anomaly over the eastern North Pacific for Z300 (Fig. S2c) but not for Z925 (Fig. S2d), illustrating that the atmospheric teleconnection is firstly established at upper levels (e.g. Ambrizzi and Hoskins 1997), where it likely triggers the feedback from the transient-eddy activity (e.g. Trenberth et al. 1998). Latitudinal shifts of the westerly jets may make the zonally-oriented Rossby waves undistinguishable (e.g. Lu et al. 2002); hence, an analysis is performed by subtracting the zonal-mean in the ensemble-mean response for geopotential height (Fig. 3-left) and streamfunction (Fig. S3) at 300 hPa. It is shown that the zonally-asymmetric circulation anomalies effectively propagate downstream into the westerly jets, thereby discarding that Rossby wave energy propagates upstream to the North Pacific. Wave activity flux diagnostic confirms that the energy propagation is eastward, off the North Atlantic jet (Fig. S4). The waveguiding time-scale in SPEEDY, of less than a week, is consistent with previous evidence from observational (Watanabe 2004), linear baroclinic model (Watanabe and Jin 2004), and comprehensive AGCM (Li 2006) results. Figure 4a summarizes how the wave perturbation at 40°N propagates downstream and amplifies with integration time, whereas Fig. 4b shows that the propagating zonally-asymmetric circulation anomalies are not an artefact of the residual operator.

At day 8 of integration (Fig. 2g, h), two centres of action over the North Pacific basin are noticeable in the ensemble-mean response at the upper troposphere. The barotropic centre of action at the exit-region of the North Pacific jet has increased in amplitude (cf. to Fig. 2e, f), indicating that it is not only sustained against dissipation but amplified, by likely extracting energy from the mean-flow on top of the wave energy propagation (Fig. S4f). 2 days after (day 10), it keeps growing (Fig. 2i, j). Recall that the baroclinic processes in the North Atlantic (Fig. 3j) are the main source for the conversion of available potential energy into kinetic energy. In the Euro-Atlantic sector the ensemble-mean atmospheric anomalies are overall stronger. The upper-tropospheric circulation anomaly over Europe has further displaced eastward and the centre of action at North Atlantic mid-latitudes has apparently splitted in two (Fig. 2i); note that these anomalies correspond to the zonal propagation/advection of the baroclinic perturbation (Figs. 2j, 5c). Together, the wavenumber-5 structure of the ensemble-mean response for Z300 embedded in the westerly jets at day 10 of integration (Fig. 2i) is already reminiscent of the quasi-equilibrium response (see Fig. 6a) and projects on the simulated NAO/CWP pattern (Fig. 1b; spatial correlation of 0.41).

Besides, the ensemble-mean response yields positive circulation anomalies at high latitudes of the North Atlantic,

Fig. 2 (*Shading/thin contours*) Ensemble-mean response for geopotential height at 300 hPa (Z300, m; *left*) and 925 hPa (Z925, m; *right*) every 2 days of integration. (*Thick contours*) Overplotted is the ensemble-mean monthly-mean zonal wind at 300 hPa ($c_i = 10 \text{ ms}^{-1}$ starting in 20 ms^{-1}) from the control run

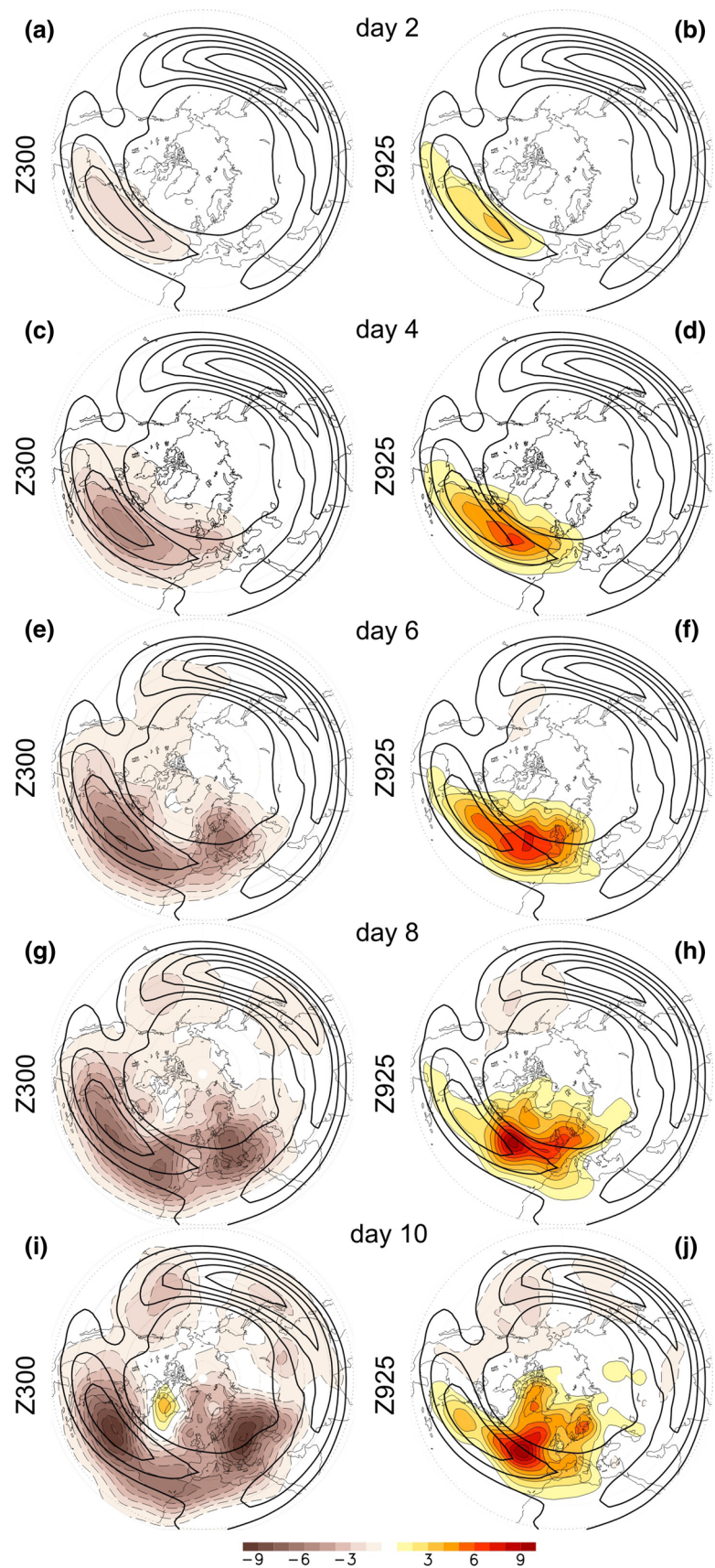
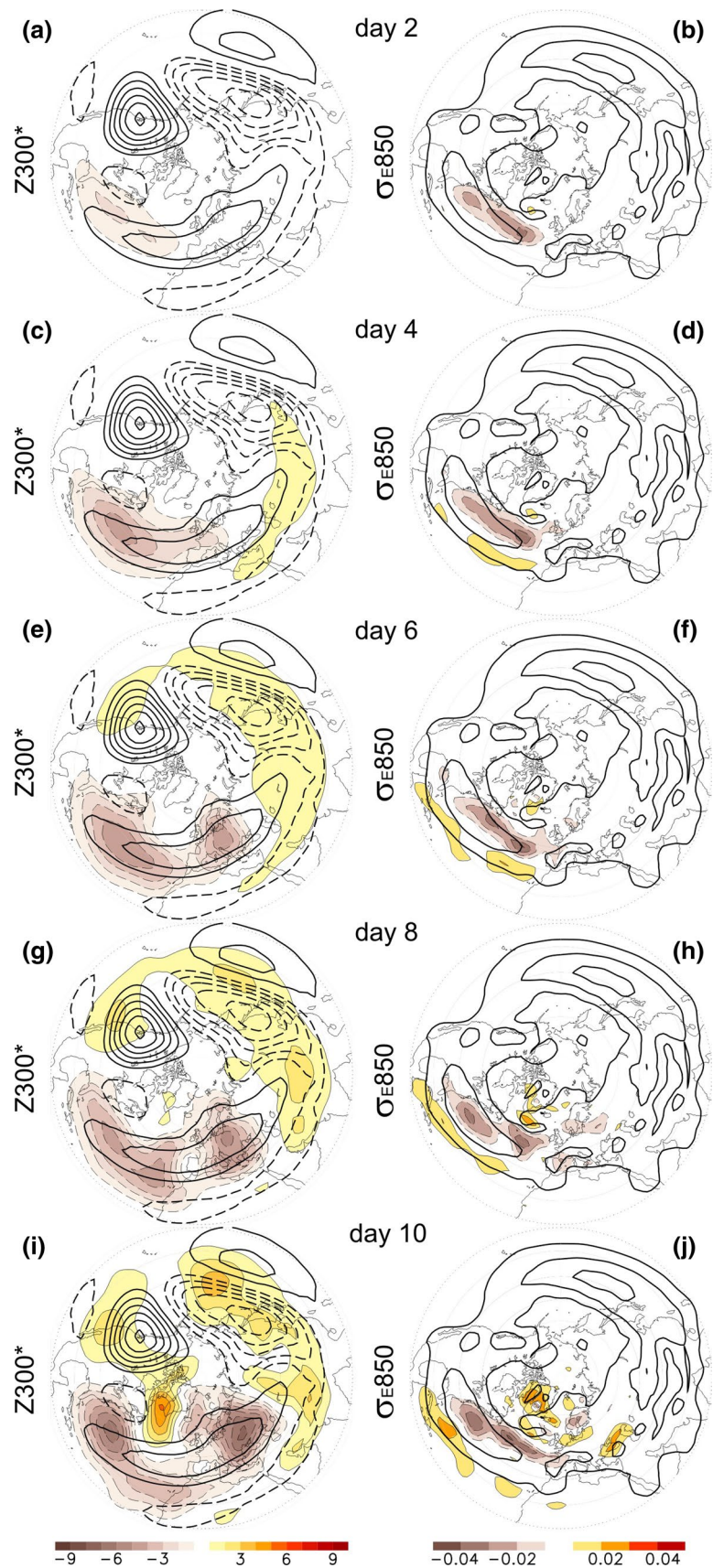


Fig. 3 (Shading/thin contours) Ensemble-mean response for the asymmetric part, i.e. departure from zonal-mean, of geopotential height at 300 hPa (Z_{300}^* , m; *left*) and Eady growth rate at 850 hPa (σ_{E850} , day^{-1} ; *right*) every 2 days of integration; σ_{E850} has been computed from potential temperature and zonal wind at 925 and 700 hPa. (Thick contours) Overplotted in each panel is the ensemble-mean monthly-mean of the corresponding field from the control run: Z_{300}^* ($c_i = 50$ m; *left*) and σ_{E850} ($c_i = 0.3$ day^{-1} ; *right*)



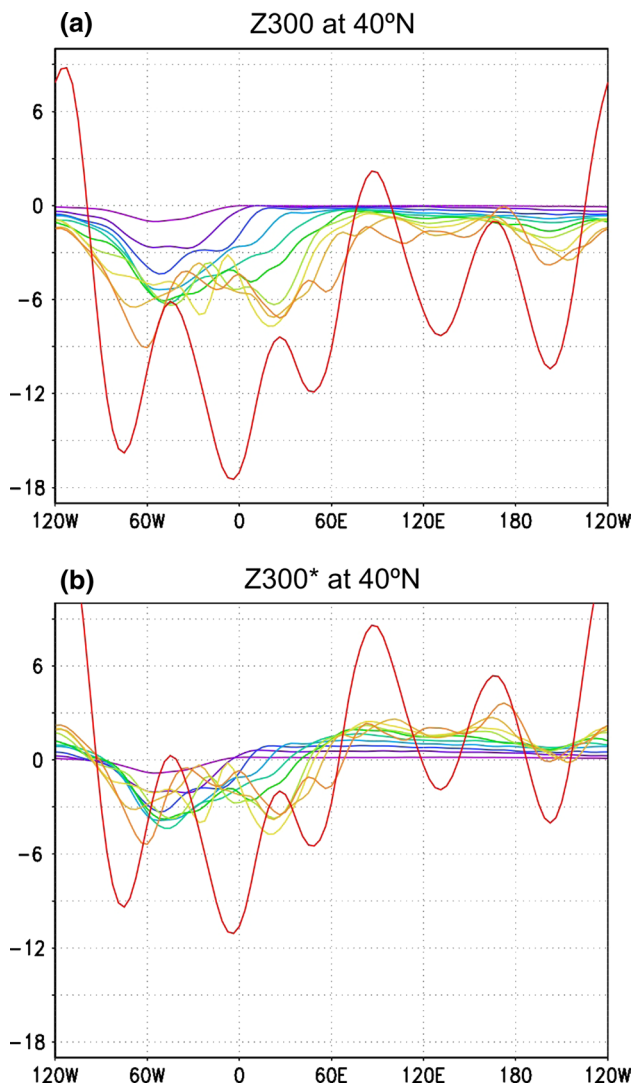


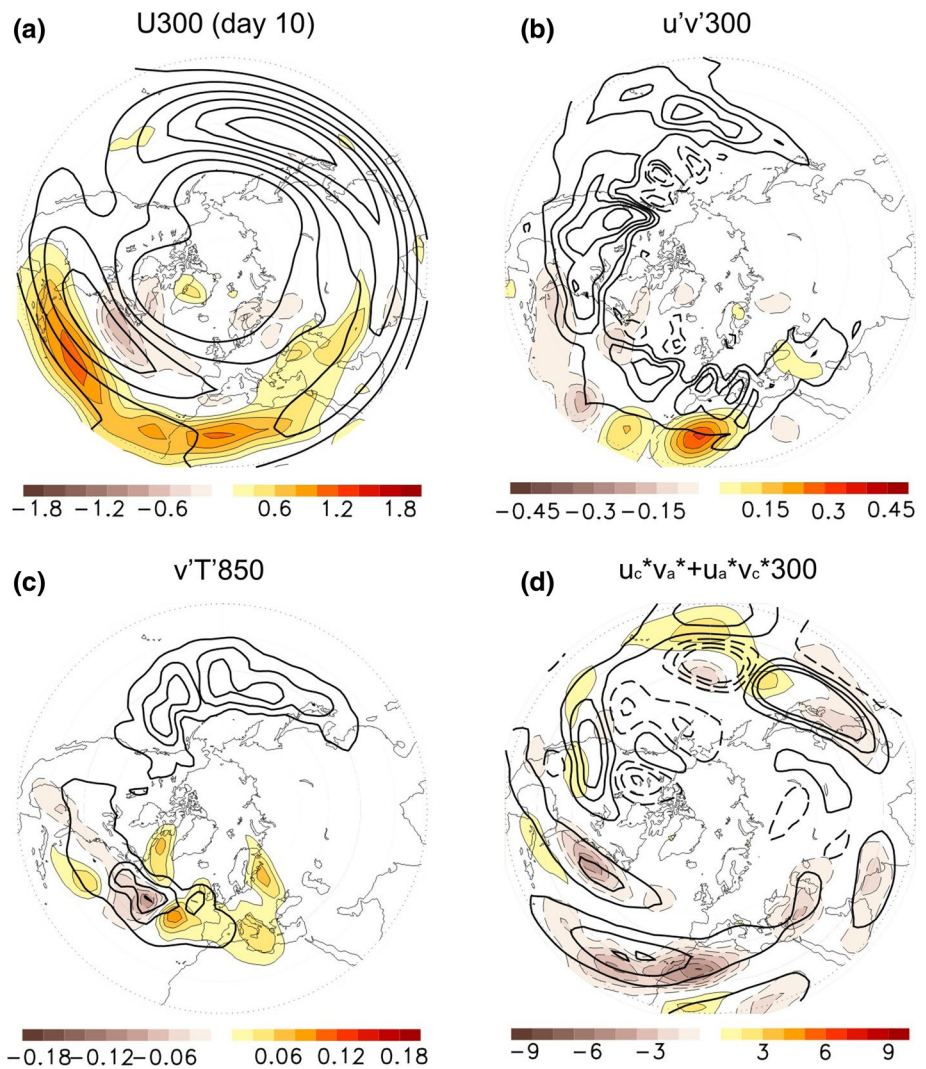
Fig. 4 Ensemble-mean response for geopotential height at 300 hPa (Z300, m; **a**) and its asymmetric part (Z300*, m; **b**), i.e. departure from zonal-mean, at 40°N every day of integration from 1 (purple) to 10 (orange), plus the averaged over the days 15–30 (red)

pointing out the first hint of a barotropic NAO-like pattern (Fig. 2i, j). This anticyclonic anomaly is located over the Greenland-blocking region, usually associated with wave-breaking on the poleward side of the storm-track/jetstream and negative NAO regime (e.g. Woollings et al. 2008, 2010; Davini et al. 2012). This mechanism could be at play according to the Eady growth rate anomalies that identify there a region of increasingly unstable flow over the days 8–10 of integration (Fig. 3h, j; Rivière and Orlanski 2007), since this perturbation would break and dissipate leading to local barotropic energy conversion (e.g. Strong and Magnusdottir 2008). The analysis of the transient-eddy heat flux, which is proportional to the vertical component of the Eliassen-Palm flux (e.g. Andrews et al. 1987), confirms

that there is an injection of wave activity over the region (Fig. 5c; Magnusdottir and Haynes 1996). The emerging barotropic structure at day 10 is accompanied by a southward displacement of the eddy-driven jet (Fig. 5a), consistent with the settling of the negative NAO phase (e.g. Woollings et al. 2010). In agreement with this latitudinal shift in the zonal wind, there are negative anomalies of transient-eddy momentum flux over the western North Atlantic (Fig. 5b), indicating that the westerly flow is being decelerated. The positive anomalies of transient-eddy momentum flux over the eastern North Atlantic (Fig. 5b) depict westerly momentum deposition that tends to accelerate the North African jet (Fig. 5a). Likewise, the dipole-like anomaly of transient-eddy heat flux at the core-region of the North Atlantic jet (Fig. 5c) implies that the storm-track is weakened and shifted to the south, as also expected during the negative NAO phase (e.g. Hurrell et al. 2003). Interestingly, the ensemble-mean response at day 10 of integration does not show large anomalies of transient-eddy/mean-flow interaction in the North Pacific basin, in agreement with the dominant linear, barotropic Rossby wave propagation (e.g. Ambrizzi and Hoskins 1997). Even so, other dynamics may be at work in the interaction between the NAO-related anomalous Rossby wavetrain and the mean-flow. Figure 3-left shows that the zonally-asymmetric Z300 anomalies are out-of-phase with the climatological wave pattern over Eurasia and the western-central North Pacific, as well as over the North Atlantic. The associated zonal-eddy momentum flux (Fig. 5d; e.g. DeWeaver and Nigam 2000a) shows overall negative anomalies in the three areas, and in particular over the former. This suggests that zonal-eddy coupling could contribute, against dissipation, to the remote atmospheric response by extracting energy from the mean-flow.

At the quasi-equilibrium stage, average of days 15–30 of integration, the circumglobal response is fully established, and the amplitude of the ensemble-mean Z300 anomalies has increased substantially (cf. Figs. 4a, 6a; spatial correlation with Fig. 1b of 0.59). Note that the two centres of action along the North Atlantic jet are stronger than any other at the upper troposphere. The wavenumber-5 structure of the ensemble-mean response, showing a non-annular pattern trapped into the westerly jets, is better illustrated by the meridional component of the wind at 300 hPa (Fig. 6b). The waveguided circulation yields a deep barotropic anomaly at the exit-region of the North Pacific jet, which represents the stronger centre of action of Z925 at mid-latitudes (Fig. 6c); this is collocated with a relative maximum of the perturbation kinetic energy (Fig. 6d), which encapsulates transient-eddy activity in the storm-tracks (e.g. Hoskins et al. 1983). The quasi-equilibrium response for Z925 over the North Atlantic (Fig. 6c) does not entirely resemble the model NAO pattern (Fig. 1d), because of the shortness of

Fig. 5 (Shading/thin contours) Ensemble-mean response at day 10 of integration for zonal wind at 300 hPa (U300, ms^{-1} ; **a**), transient-eddy momentum flux at 300 hPa ($u'v'300$, $\text{m}^2 \text{s}^{-2}$; **b**), transient-eddy heat flux at 850 hPa ($v'T'850$, $\text{ms}^{-1} \text{K}$; **c**), and zonal-eddy momentum flux at 300 hPa ($u_c^*v_a^* + u_a^*v_c^*300$, $\text{m}^2 \text{s}^{-2}$; **d**); the latter computed from the climatological stationary wave (u_c^* , v_c^*) and daily anomalous zonal-eddy components (u_a^* , v_a^*). All eddy covariances have been averaged over the days 8–10 of integration. (Thick contours) Overplotted in each panel is the ensemble-mean monthly-mean of the corresponding field from the control run: U300 ($ci = 10 \text{ ms}^{-1}$ starting in 20 ms^{-1} ; **a**), $u'v'300$ ($ci = 5 \text{ m}^2 \text{ s}^{-2}$; **b**), $v'T'850$ ($ci = 2.5 \text{ ms}^{-1} \text{K}$; **c**), and $u_c^*v_c^*300$ (at ± 20 , ± 60 , $\pm 100 \text{ m}^2 \text{ s}^{-2}$; **d**); with $u'v'300$ and $v'T'850$ computed from filtered daily data using the 24 h-difference filter (e.g. Wallace et al. 1988; Chang and Fu 2002)



the integration (see Sect. 2; Fig. S5), but transient-eddy activity/feedback (Fig. 6d) has been efficient enough to start setting the barotropic dipole-like pattern, as compared to day 10 (Fig. 2i, j), particularly over eastern North America-Iberian Peninsula at mid-latitudes and over Greenland-Scandinavian Peninsula at subpolar latitudes (Fig. 6a, c).

5 Summary and discussion

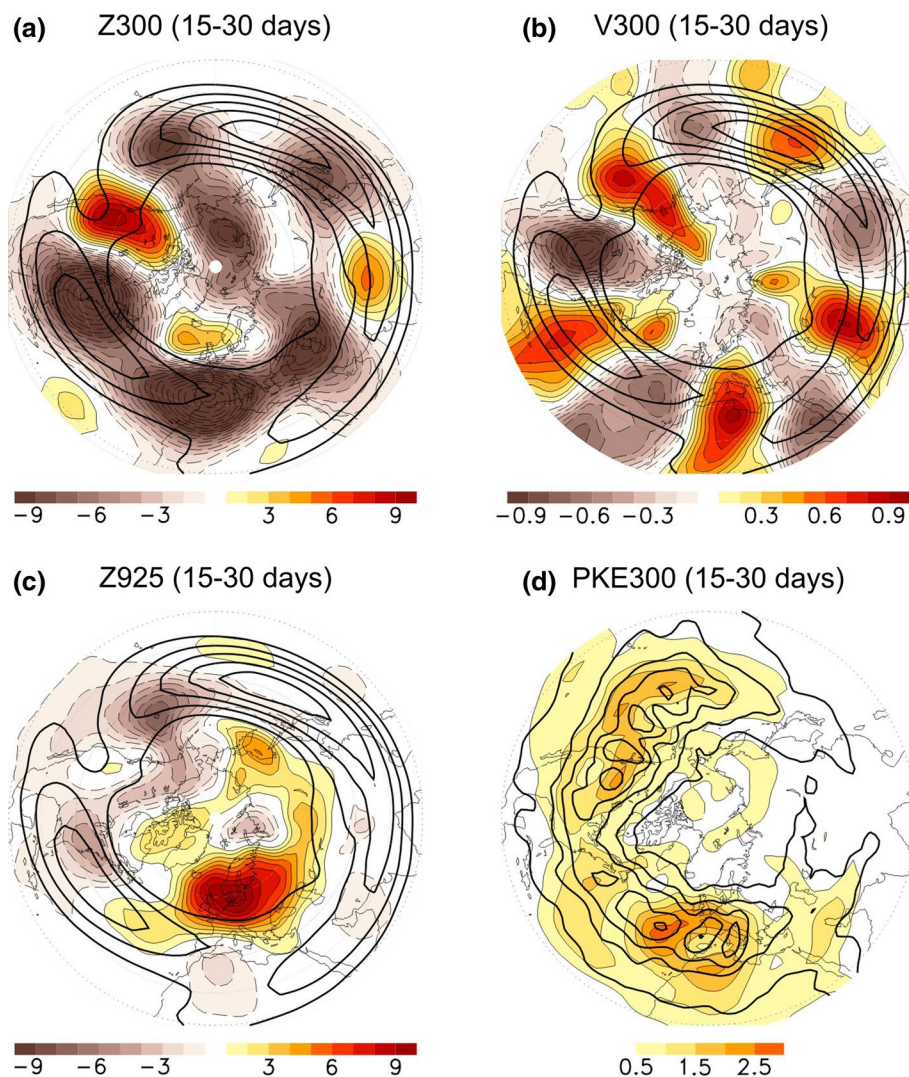
The temporal development of the NAO-related circum-global response to extratropical North Atlantic SSTs, with the transition from a linear Rossby wave response towards a nonlinear response including transient-eddy feedbacks, has been investigated with SPEEDY-AGCM simulations under perpetual January conditions.

The results shown here support the hypothesis that the hemispheric signature of the winter NAO at surface, particularly the associated circulation anomalies over the

North Pacific basin, could be explained by tropospheric dynamics (without the need of interaction with the stratosphere) involving a Rossby wavetrain channelized into the westerly jets, which is consistent with the CWP pattern at the upper troposphere (e.g. García-Serrano et al. 2011). The resemblance of this waveguided, non-annular teleconnection to the observational and model NAO-related upper-tropospheric wavenumber-5 structure suggests that NAO/CWP-like variability may represent a natural mode of atmospheric variability (Branstator 2002; Branstator and Selten 2009).

The findings also imply that the mid-latitude North Pacific and North Atlantic centres of action in the hemispheric NAO signature do not fluctuate in phase, in agreement with the idea that no longitudinal coherence in transient-eddy activity is expected (e.g. Vallis and Gerber 2008; Gerber and Vallis 2009; Wettstein and Wallace 2010); thereby, the NAO/CWP paradigm is in contrast with the AO/NAM paradigm, where a large-scale, hemispheric

Fig. 6 (Shading/thin contours) Ensemble-mean response averaged over the days 15–30 of integration for geopotential height at 300 hPa (Z300, m; **a**), meridional wind at 300 hPa (V300, ms^{-1} ; **b**), geopotential height at 925 hPa (Z925, m; **c**), and perturbation kinetic energy at 300 hPa ($\text{PKE300} = (u'u' + v'v')/2$, $\text{m}^2 \text{s}^{-2}$; **d**); the eddy covariances have been averaged over the days 15–30 of integration. (Thick contours) Overplotted is the ensemble-mean monthly-mean zonal wind at 300 hPa ($c_i = 10 \text{ ms}^{-1}$ starting in 20 ms^{-1} ; **a–c**) and PKE300 ($c_i = 45 \text{ m}^2 \text{ s}^{-2}$; **d**) from the control run; the latter computed from filtered daily data using the 24 h-difference filter (e.g. Wallace et al. 1988; Chang and Fu 2002)



seesaw between middle and high latitudes is postulated. However, the NAO/CWP-like variability does not revoke the AO/NAM pattern, but instead provides a dynamical framework to consistently understand its quasi-zonally symmetric appearance at surface. From this perspective, the AO would correspond to the circumglobal extension of the more regional NAO (c.f. Kimoto et al. 2001). The NAO/CWP could also explain why the mode of variability in the Northern Hemisphere appears to be dominated by atmospheric variability in the Atlantic sector (e.g. Thompson et al. 2003). It could well help to settle a unifying view of the NAO-AO variability, which is much-needed due to its important environmental impacts and implication for climate forecasting.

Targeted modelling efforts are required to provide further support to the dynamical framework discussed here. Exploration could point at analysing the downstream

propagation of NAO-related atmospheric anomalies, in the North Atlantic, induced by tropospheric mean-flow instabilities (e.g. Watanabe 2009) and/or changes in the stratospheric polar vortex strength (e.g. Garfinkel et al. 2013). Theoretical understanding of the predominance of wave-number-5 in the CWP might also be subject of research (see last paragraph in Sect. 3).

Acknowledgments This work has been partially supported by the CANON Foundation in Europe (Grant 2011-062). JG-S was partially supported by the H2020-funded MSCA-IF-EF DPETNA project (GA No. 655339). Thanks to Mashiro Watanabe and Masato Mori (AORI, University of Tokyo) for useful discussions in the early stages of this study. Thanks also to Francisco J. Doblas-Reyes (BSC, Spain) and Pablo Zurita-Gotor (UCM, Spain) for their help during the review process. Technical support at BSC (Computational Earth Sciences group) is sincerely acknowledged. The authors are grateful to the anonymous reviewers for their encouragement and helpful suggestions.

References

- Ambaum MHP, Hoskins BJ (2002) The NAO troposphere-stratosphere connection. *J Clim* 15:1969–1978
- Ambaum MHP, Hoskins BJ, Stephenson DB (2001) Arctic oscillation or North Atlantic Oscillation? *J Clim* 14:3495–3507
- Ambrizzi T, Hoskins BJ (1997) Stationary Rossby-wave propagation in a baroclinic atmosphere. *Q J R Meteorol Soc* 123:919–928
- Andrews DG, Holton JR, Leovy CB (1987) Middle atmospheric dynamics. Academic Press, London
- Annamalai H, Okajima H, Watanabe M (2007) Possible impact of the Indian Ocean SST on the Northern Hemisphere circulation during El Niño. *J Clim* 20:3164–3189
- Baldwin MP, Dunkerton TJ (2001) Stratospheric harbingers of anomalous weather regimes. *Science* 294:581–584
- Baldwin MP, Cheng X, Dunkerton TJ (1994) Observed correlations between winter-mean tropospheric and stratospheric circulation anomalies. *Geophys Res Lett* 21:1141–1144
- Baldwin MP, Stephenson DB, Thompson DJ, Dunkerton TJ, Charlton AJ, O'Neill A (2003) Stratospheric memory and skill of extended-range weather forecasts. *Science* 301:636–640
- Bleck R, Rooth C, Smith LT (1992) Salinity-driven thermocline transients in a wind- and thermohaline-forced isopycnal coordinate model of the North Atlantic. *J Phys Oceanogr* 22:1486–1505
- Bracco A, Kucharski F, Kallummal R, Molteni F (2004) Internal variability, external forcing, and climate trends in multi-decadal AGCM ensembles. *Clim Dyn* 23:659–678
- Branstator G (2002) Circum global teleconnections, the jetstream waveguide, and the North Atlantic Oscillation. *J Clim* 15:1893–1910
- Branstator G, Selten F (2009) “Modes of variability” and climate change. *J Clim* 22:2639–2658
- Chang EKM, Fu Y (2002) Interdecadal variations in Northern Hemisphere winter storm track intensity. *J Clim* 15:642–658
- Christiansen B (2002) On the physical nature of the Arctic Oscillation. *Geophys Res Lett*. doi:10.1029/2002GL015208
- Cohen J, Saito K (2002) A test for annular modes. *J Clim* 15:2537–2546
- Davini P, Cagnazzo C, Neale R, Tribbia J (2012) Coupling between Greenland blocking and the North Atlantic Oscillation pattern. *Geophys Res Lett* 39:L14701. doi:10.1029/2012GL052315
- Davini P, Cagnazzo C, Anstey JA (2014) A blocking view of the stratosphere-troposphere coupling. *J Geophys Res Atmos*. doi:10.1002/2014JD021703
- Deser C (2000) On the teleconnectivity of the “Arctic Oscillation”. *Geophys Res Lett* 27:779–782
- Deser C, Tomas RA, Peng S (2007) The transient atmospheric circulation response to North Atlantic SST and sea ice anomalies. *J Clim* 20:4751–4767
- DeWeaver E, Nigam S (2000a) Do stationary waves drive the zonal-mean jet anomalies of the northern winter? *J Clim* 13:2160–2176
- DeWeaver E, Nigam S (2000b) Zonal-eddy dynamics of the North Atlantic Oscillation. *J Clim* 13:3893–3914
- Dommenges D, Latif M (2002) A cautionary note on the interpretation of EOFs. *J Clim* 15:216–225
- Feldstein SB, Franzke C (2006) Are the North Atlantic Oscillation and the Northern Annular Mode distinguishable? *J Atmos Sci* 63:2915–2930
- Ferreira D, Frankignoul C (2005) The transient atmospheric response to midlatitude SST anomalies. *J Clim* 18:1049–1067
- García-Serrano J, Rodríguez-Fonseca B, Bladé I, Zurita-Gotor P, de la Cámara A (2011) Rotational atmospheric circulation during North Atlantic-European winter: the influence of ENSO. *Clim Dyn* 37:1727–1743
- Garfinkel CI, Waugh DW, Gerber EP (2013) The effect of tropospheric jet latitude on coupling between the stratospheric polar vortex and the troposphere. *J Clim* 26:2077–2095
- Gerber EP, Vallis GK (2009) On the zonal structure of the North Atlantic Oscillation and annular modes. *J Atmos Sci* 66:332–352
- Haarsma RJ, Campos EJD, Hazeleger W, Severijns C, Piola AR, Molteni F (2005) Dominant modes of variability in the South Atlantic: a study with a hierarchy of ocean-atmosphere models. *J Clim* 18:1719–1735
- Haarsma RJ, Campos EJD, Hazeleger W, Severijns C (2008) Influence of the meridional overturning circulation on tropical Atlantic climate and variability. *J Clim* 21:1403–1416
- Hazeleger W, Haarsma RJ (2005) Sensitivity of tropical Atlantic climate to mixing in a coupled ocean-atmosphere model. *Clim Dyn* 25:387–399
- Hazeleger W, Severijns C, Haarsma RJ, Selten F, Sterl A (2003) SPEEDO-model description and validation of a flexible coupled model for climate studies. KNMI Tech Rep TR-257, KNMI, De Bilt, Netherlands
- Hoskins BJ, Ambrizzi T (1993) Rossby wave propagation on a realistic longitudinally varying flow. *J Atmos Sci* 50:1661–1671
- Hoskins BJ, Valdes PJ (1990) On the existence of storm-tracks. *J Atmos Sci* 47:1854–1864
- Hoskins BJ, James IN, White GH (1983) The shape, propagation and mean-flow interaction of large-scale weather systems. *J Atmos Sci* 40:1595–1612
- Hsu H-H, Lin S-H (1992) Global teleconnections in the 250-mb streamfunction field during the North Hemisphere winter. *Mon Wea Rev* 120:1169–1190
- Hurrell JW, Deser C (2009) North Atlantic climate variability: the role of the North Atlantic Oscillation. *J Mar Syst* 78:28–41
- Hurrell JW, Kushnir Y, Ottensen G, Visbeck M (2003) An overview of the North Atlantic Oscillation. In: *The North Atlantic Oscillation—climatic significance and environmental impact*. AGU Geophys Monogr 134:1–36
- Huth R (2006) Pacific centre of the Arctic Oscillation: product of high local variability rather than teleconnectivity. *Tellus* 58A:601–604
- Kimoto M, Jin F-F, Watanabe M, Yasutomi N (2001) Zonal-eddy coupling and a neutral mode theory for the Arctic Oscillation. *Geophys Res Lett* 28:737–740
- Kindem IT, Christiansen B (2001) Tropospheric response to stratospheric ozone loss. *Geophys Res Lett* 28:1547–1550
- King MP, Kucharski F, Molteni F (2010) The roles of external forcings and internal variabilities in the Northern Hemisphere atmospheric circulation change from the 1960s to the 1990s. *J Clim* 23:6200–6220
- Kucharski F, Molteni F (2003) On non-linearities in a forced North Atlantic Oscillation. *Clim Dyn* 21:677–687
- Kucharski F, Molteni F, King MP, Farneti R, Kang I-S, Feudale L (2013) On the need of intermediate complexity general circulation models: a “SPEEDY” example. *Bull Amer Meteor Soc* 94:25–30
- Li LZ (2006) Atmospheric GCM response to an idealized anomaly of the Mediterranean sea surface temperature. *Clim Dyn* 27:543–552
- Li LZ, Conil S (2003) Transient response of an atmospheric GCM to North Atlantic SST anomalies. *J Clim* 16:3993–3998
- Lu R-Y, Oh J-H, Kim B-J (2002) A teleconnection pattern in upper-level meridional wind over the North African and Eurasian continent in summer. *Tellus* 54A:44–55
- Magnusdottir G, Haynes PH (1996) Wave activity diagnostics applied to baroclinic wave life cycles. *J Atmos Sci* 53:2317–2353
- Molteni F (2003) Atmospheric simulations using a GCM with simplified physical parametrizations. I: model climatology and variability in multi-decadal experiments. *Clim Dyn* 20:175–191
- Nigam S (2003) Teleconnections. In: Holton JR, Pyle JA, Curry JA (eds) *Encyclopedia of atmospheric sciences*. Academic Press, Elsevier Science, pp 2243–2269

- Norton WA (2003) Sensitivity of Northern Hemisphere surface climate to simulation of the stratospheric polar vortex. *Geophys Res Lett* 30 doi:[10.1029/2003GL016958](https://doi.org/10.1029/2003GL016958)
- Perlwitz J, Graf H-F (1995) The statistical connection between tropospheric and stratospheric circulation of the Northern Hemisphere in winter. *J Clim* 8:2281–2295
- Rivière G, Orlanski I (2007) Characteristics of the Atlantic storm-track eddy activity and its relation with the North Atlantic Oscillation. *J Atmos Sci* 64:241–266
- Shaw TA, Perlwitz J, Weiner O (2014) Troposphere-stratosphere coupling: links to North Atlantic weather and climate, including their representation in CMIP5 models. *J Geophys Res Atmos* 119:5864–5880
- Smith TM, Reynolds RW, Peterson TC, Lawrimore J (2008) Improvements to NOAA's historical merged land-ocean surface temperature analysis (1880–2006). *J Clim* 21:2283–2296
- Strong C, Magnusdottir G (2008) Tropospheric Rossby wave breaking and the NAO/NAM. *J Atmos Sci* 65:2861–2876
- Thompson DWJ, Wallace JM (1998) The Arctic Oscillation signature in the wintertime geopotential height and temperature fields. *Geophys Res Lett* 25:1297–1300
- Thompson DWJ, Wallace JM (2000) Annular modes in the extratropical circulation. Part I: month-to-month variability. *J Clim* 13:1000–1016
- Thompson DWJ, Wallace JM (2001) Regional climate impacts of the Northern Hemisphere annular mode. *Science* 293:85–89
- Thompson DWJ, Lee S, Baldwin MP (2003) Atmospheric processes governing the Northern Hemisphere Annular Mode/North Atlantic Oscillation. In: *The North Atlantic Oscillation—climatic significance and environmental impact*. AGU Geophys Monogr 134:81–112
- Trenberth KE, Branstator G, Karoly D, Kumar A, Lau N-C, Ropelewski C (1998) Progress during TOGA in understanding and modeling global teleconnections associated with tropical seas surface temperatures. *J Geophys Res* 103:14291–14324
- Uppala SM et al (2005) The ERA-40 re-analysis. *Q J R Meteorol Soc* 131:2961–3012
- Vallis GK, Gerber EP (2008) Local and hemispheric dynamics of the North Atlantic Oscillation, annular patterns and the zonal index. *Dyn Atmos Ocean* 44:184–212
- von Storch H, Zwiers FW (2001) *Statistical analysis in climate research*. Cambridge University Press, UK
- Wallace JM (2000) North Atlantic Oscillation/annular mode: two paradigms-one phenomenon. *Q J R Meteorol Soc* 126:791–805
- Wallace JM, Thompson DW (2002) The Pacific center of action of the Northern Hemisphere Annular Mode: real or artifact? *J Clim* 15:1987–1991
- Wallace JM, Lim G-H, Blackmon ML (1988) Relationship between cyclone tracks, anticyclone tracks and baroclinic waveguides. *J Atmos Sci* 45:439–462
- Watanabe M (2004) Asian jet waveguide and downstream extension of the North Atlantic Oscillation. *J Clim* 17:4674–4691
- Watanabe M (2009) Self-limiting feedback between baroclinic waves and a NAO-like sheared zonal flow. *Geophys Res Lett* 36:L08803. doi:[10.1029/2009GL037176](https://doi.org/10.1029/2009GL037176)
- Watanabe M, Jin F-F (2004) Dynamical prototype of the Arctic Oscillation as revealed by a neutral singular vector. *J Clim* 17:2119–2138
- Wettstein JJ, Wallace JM (2010) Observed patterns of month-to-month storm-track variability and their relationship to the background flow. *J Atmos Sci* 67:1420–1437
- Woollings T, Hoskins BJ, Blackburn M, Berrisford P (2008) A new Rossby wave-breaking interpretation of the North Atlantic Oscillation. *J Atmos Sci* 65:609–626
- Woollings T, Hannachi A, Hoskins BJ, Turner A (2010) A regime view of the North Atlantic Oscillation and its response to anthropogenic forcing. *J Clim* 23:1291–1307